Investigation of Welding Residual Stress of High Tensile Steel by Finite Element Method and Experiment

Chang-Sung Seok*, Myung-Won Suh* and Ji-Hong Park**

(Received October 29, 1998)

Due to varying temperature distribution of welding area during welding process, thermal stress is generated. It is known that the thermal stress forms residual stress. The welding residual stress has an important effect on welding deformation, embrittlement fracture, fatigue fracture, etc. In this paper, residual stress due to welding was numerically investigated by finite element method. To verify the results of numerical analysis, the residual stress of high tensile steel was measured by the hole-drilling method. Temperature change experimentally measured at the location of 3-mm-off-weld-bead, in addition, was compared with the numerical analysis. The above methodologies were applied to H-plate with 13.5mm thickness through MIG welding process. The distributions of the residual stress and the temperature distributions from the experimental and the numerical analyses were confirmed to be close.

Key Words : Welding Joint, Finite Element Method, Residual Stress

1. Introduction

Davy discovered electronic arc in 1801, and Benardos, scientist of the U. S. S. R., invented welding method using a super-heat of carbon arc in 1887. Since Slowjanow invented modern arc welding method, welding technique made rapid progress(Park, 1994). Due to the development of welding technique, the application area of welding, such as architecture, bridge, shipbuilding, automobile, atomic reactor, and even the houseware is getting wider.

Welding has the advantages of high joint efficiency, simple structure, curtailment of expenditure and flexibility for the joint method. The disadvantages of the welding are the eminent change of the quality of the material, deformation, shrinkage and residual stress(Park, 1994).

During welding, nonuniform temperature is distributed around welding area by means of local heating. The nonuniform temperature distribution generates thermal stress. As the temperature of base metal rises, yield stress decreases and thermal stress increases(Yang et al., 1991). It is known that such welding residual stress has an important influence on welding deformation, fatigue fracture, embrittlement fracture, buckling strength, and etc.

There are various methods in evaluating the distribution of the residual stresses. In the category of the experimental method, there are nondestructive methods such as X-ray diffraction and ultrasonic method and destructive methods like hole drilling method, Gunnert method and sectioning method. Hole drilling method, which was proposed by Mather in 1934, is most widely used for its simplicity and accuracy(Jeon, 1989).

For the case of nonuniform stress around hole, Kabiri(1986) obtained more exact solution by integrating the infinitesimal strain over the area of strain gage. Schajer(1981) proposed new relaxation coefficients which vary through the depth and proved that the strains relaxed in blind-hole and those in through-hole are not identical.

The trials to perform detailed analysis of welding residual stress have increased considerably during the last two decades owing to the development of computers and the numerical methods, such as the finite element method(Getnarski, 1986). Hibitt and Marcall(1973) constructed

* School of Mechanical Engineering, SungKyunKwan Univ., Suwon, Korea.
** LG Industrial System.

numerical thermo-mechanical model using finite element method. Roeleus et al. (1994) investigated the influence of the mechanical coupling terms on the temperature field and found that this influence is negligible. Roelens, Maltrud and Lu (1994) compared experimental results of X-ray diffraction method with the result of numerical analysis on welding residual stress distributed in the cross section of 30mm thick A52 steel. For the complete finite element analysis of welding residual stress, it is known that further researches are necessary to secure material properties such as thermal conductivity, heat capacity, modulus of elasticity, yield limit, and Poisson's ratio for the wide range of temperature being experienced during welding process (Getnarski, 1986).

In this research, the finite element method and hole drilling method are applied to H-plate with 13.5 mm thickness through 4-pass MIG welding. Those results are compared.

2. Finite Element Analysis

The geometry of butt weld joint (H-plate) made of high tensile steel is depicted in Fig. 1. Welding process and weld design are expressed at the cross section of H-plate as shown in Fig. 2. Weld is designed as X-groove and 4-pass. In the figure, the numbers ①~④ denote the procedure of the 4-pass weld. Mesh for the finite element analysis of H-plate is constructed as shown in Fig. 3. The chemical composition and material property of base metal and weld metal is shown in Table 1 and Table 2. The process of 4-pass weld is simulated by applying to total welding time and heat flux of each pass discribed in Table 3. Figure 4 shows one pass of heat flux imposed in the successive welding process. The values of parameter t_1, t_2, t_3, t_4 and q in Fig. 4 are calculated from Table 3 to simulate each pass. It is assumed

Table 1 Chemical composition of high tension steel.

	Composition (Weight percent : %)							
	C	Mn	Si	P	S	Ni	Cr	Mo
Base metal	0.19	0.25	0.2	0.006	0.005	2.96	1.45	0.37
Weld metal	0.05	1.61	0.28	0.006	0.002	1.66	0.11	0.34

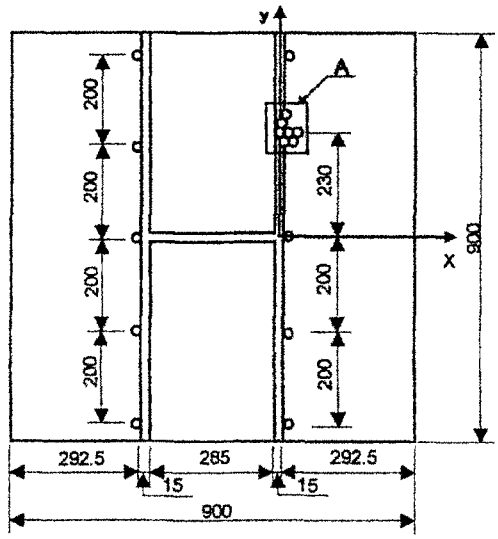

(a) H-plate

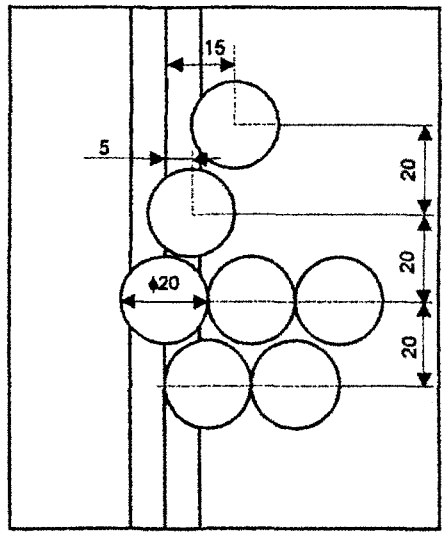

(b) Detail of 'A'

Fig. 1 H-plate and the location of strain gages

Table 2 Mechanical properties of high tension steel.

	Yield strength (MPa)	U.T.S (MPa)	Elongation (%)
Base metal	1079	1177.2	15
Weld metal	572.7	654.4	2

that the pre-heat temperature is 150℃ and the final temperature is 25℃. Natural convection takes place around H-plate and convective coefficient is 4.5 W/m² · ℃. The mechanical boundary conditions are applied in order that only rigid body motion might be kept away. In other word, hinge support was applied to left end node of FEM model and roller support, right end node. Due to thermal stress problem, analysis type is coupled elastic-plastic analysis commercial code used by this analysis was ABAQUS version 5.4. The residual stresses by finite element analysis are calculated by the following procedure.

(1) Using plane strain element, finite element mesh for cross section of H-plate is constructed as in Fig. 3.

(2) Elements corresponding to weld bead are removed as shown in Fig. 5 (a).

(3) Elements corresponding to the first welding pass are generated as shown in Fig. 5 (b).

(4) Heat flux as shown in Fig. 4 is applied to the corresponding element for the first welding pass.

(5) Total elements are cooled by means of natural convection in proper time interval, as in Fig. 4. The distributions of temperature and stress at the end of the first welding pass are saved as initial conditions for the next pass.

(6) Step 3 to 5 are repeated for the rest of welding pass.

Table 3 Welding condition of H-plate.

Welding process	Total welding time (sec)	Total welding length (mm)	Heat input (J/m)
No. 1 pass	436	2133	1,912,900
No. 2 pass	557	2133	2,469,500
No. 3 pass	351	2133	1,489,000
No. 4 pass	375	2133	1,717,000

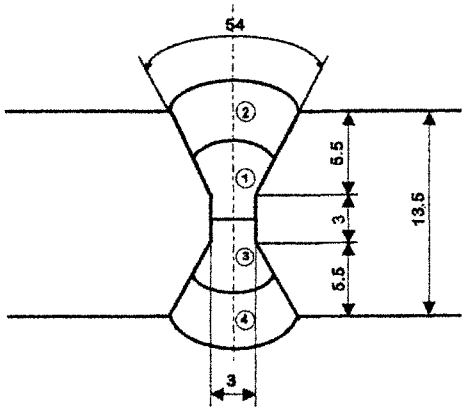

Fig. 2 Welding sequence and location of the 4-pass

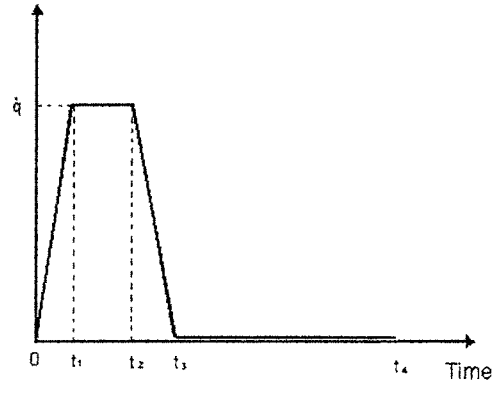

Fig. 4 Heat flux model for each pass of welding process

(a) The whole mesh

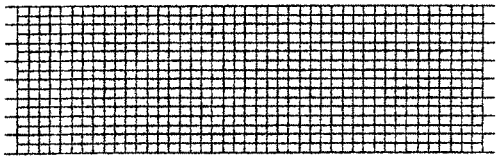

(a) The mesh for the weld zone

Fig. 3 Mesh for finite element analysis of H-plate

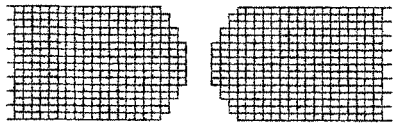

(a) The initial mesh

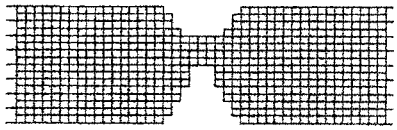

(b) The mesh for the first pass

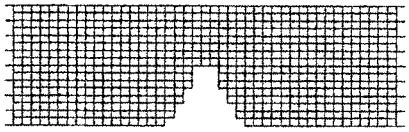

(c) The mesh for the second pass

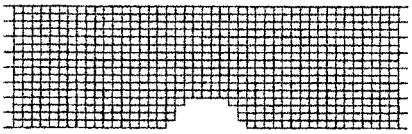

(d) The mesh for the third pass

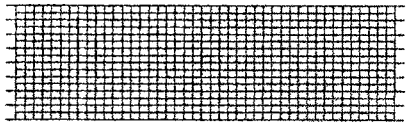

(e) The mesh for the fourth pass

Fig. 5 The shape of mesh for initial and each pass

3. Residual Stress Measurement using Hole-Drilling Method

To measure welding residual stress, strain gages are attached at the locations of 0, 5, 10, 15, 20, 30, 40mm from the center line of weld bead to the transverse direction, which is X-direction in Fig. 1. The locations of strain gage are expressed in Fig. 1. Because of the area of strain gage itself, the strain gages are not attached in a straight line.

Milling machine produced by WHASHIN Inc. and 4.5 mm end mill is used for the hole drilling. SM-600 strain gage indicator and SS-24R switch-and-balance unit manufactured by Kyowa Electronic Inc. is applied as strain-measurement instrumentation. Micro-measurements strain gage rosettes, type KFG-3-120-D28-11, is used in sensing strain.

Residual stress measurement test is performed in accordance with ASTM E837-92 (standard test method for determining residual stresses by the hole-drilling strain gage method). The diameter and the depth of hole are determined by means of the following conditions (ASTM, 1995).

$$0.3<\frac{D_0}{D}<0.5 \tag{1}$$

$$t>1.2D \qquad d=0.4D \tag{2}$$

$$t<1.2D \qquad d=t \tag{3}$$

where,

D : Diameter of strain gage circle
D_0 : Diameter of hole
t : Specimen thickness
d : Depth of hole

The surface of specimen is treated with sandpaper. Alien substance on surface of specimen is removed with alcohol. After the hole is drilled in the center of strain gage rosettes attached on specimen, the strain of specimen is relaxed. The magnitude and direction of principal stress are obtained from the measured strains by the following equations.

$$\beta=\frac{1}{2}\tan^{-1}\left(\frac{\varepsilon_3+\varepsilon_1-2\varepsilon_2}{\varepsilon_3-\varepsilon_1}\right) \tag{4}$$

$$\bar{A}=-\frac{1+\nu}{2E}\bar{a} \tag{5}$$

$$\bar{B}=-\frac{1}{2E}\bar{b} \tag{6}$$

$$\sigma_{min},\ \sigma_{max}=-\frac{(\varepsilon_3+\varepsilon_1)}{4\bar{A}} \pm\frac{\sqrt{(\varepsilon_3-\varepsilon_1)^2+(\varepsilon_3+\varepsilon_1-2\varepsilon_2)^2}}{2\bar{B}} \tag{7}$$

Where,

β : Angle measured clockwise from the location of the reference gage to the direction of σ_{max}. The reference gage for rosettes is ε_1.

ε_1, ε_2, ε_3 : Principal strains measured by experiment

$\bar{A}$, $\bar{B}$: Calibration constants

$\bar{a}$, $\bar{b}$: Dimensionless, material independent coefficients

σ_{max}, σ_{min} : Principal residual stresses The related values of the parameters in the above equations are in the reference(ASTM, 1995).

4. Results and Discussion

The longitudinal (y-direction in Fig. 1) and the transverse(x-direction in Fig. 1) components of the residual stress from numerical analysis and experiment are shown in Fig. 6 and Fig. 7. It is observed that in the case of the longitudinal component of the residual stress, the tensile residual stress increases from the center line of weld bead to 5 mm in the transverse direction and decreases to converge to zero after the location of 5 mm. That is, the maximum tensile residual stress occurs in HAZ(heat affected zone), which is the location of 5 mm apart from the center line of weld bead, and the magnitude is 62.5 % of yield stress. In the case of the transverse component of the residual stress, mainly the compressive residual stress with smaller value than that of the longitudinal component occurs.

In the comparison of numerical analysis and experiment, the longitudinal component of the residual stress shows a good agreement between the results of measurement and numerical analysis as in Fig. 6. In the case of the transverse component of the residual stress the trends of the experimental and the numerical curve are acceptable to be close except for HAZ area as shown in Fig. 7. This is thought that the discrepancy occurs due to the insufficient material data corresponding to the wide range of the temperature.

The temperature transients during the first pass at the location of 3-mm-off-weld-bead obtained by the measurement and the finite element analysis are shown in Fig. 8. For heating cycle, the numerical analysis approximates very closely the experiment. There, however, is a little difference in the case of cooling cycle. This may be caused by the deviated natural convection coefficient.

From the finite element analysis, the longitudinal and the transverse components of the residual stress along the thickness are obtained as in Fig. 9 and Fig. 10. A, B, C, D and E in the figures describe the locations, which are 0, 5, 10, 15, 20mm apart from the center line of weld bead.

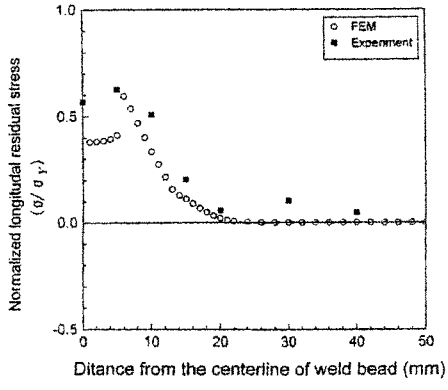

Fig. 6 The longitudinal component (y-direction in Fig. 1) of the residual stress in H-plate

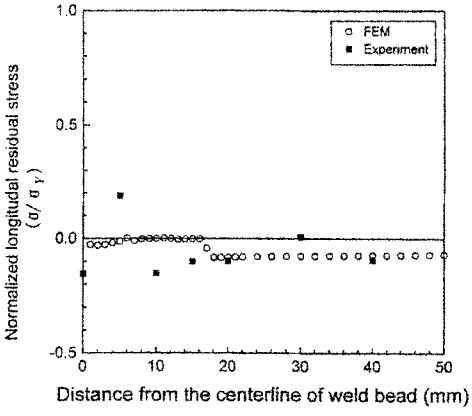

Fig. 7 The transverse component (x-direction in Fig. 1) of the residual stress in H-plate

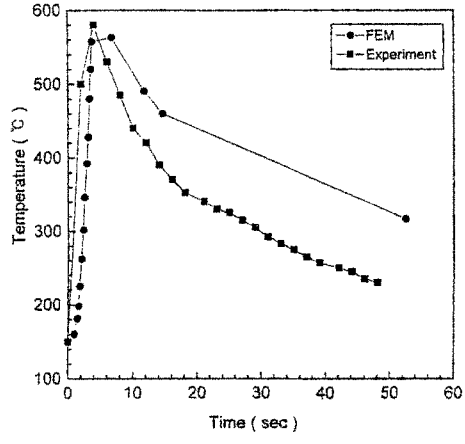

Fig. 8 Temperature change during the first pass at the location of 3-mm-off-weld-bead

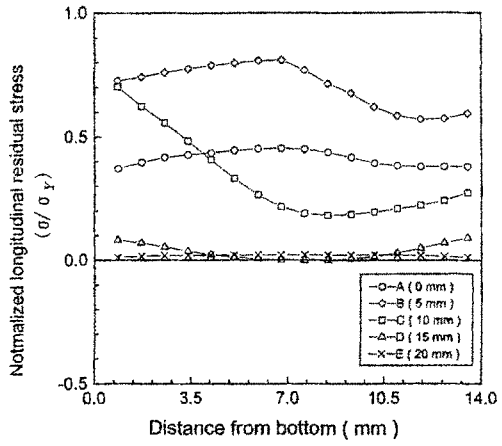

Fig. 9 The longitudinal component (y-direction in Fig. 1) of the residual stress along the thickness

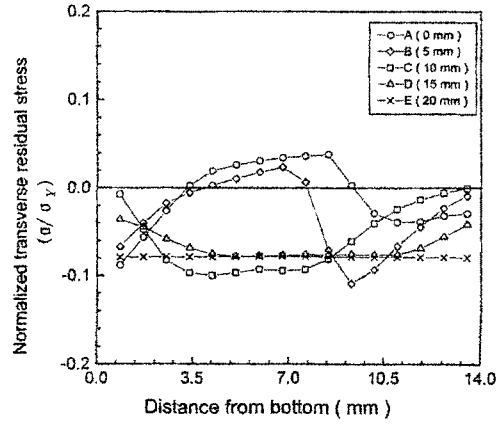

Fig. 10 The transverse component (x-direction in Fig. 1) of the residual stress along the thickness

The location of A and B are corresponding to the weldment and HAZ, respectively. In addition, C, D, E are for the base metal.

In the case of the longitudinal component of the residual stress, the tensile residual stresses of locations of A and B reach the maximum values in the middle of thickness of H-plate as in Fig. 9. It is observed that the residual stress distribution of B(HAZ) is higher than that of A(weldment). The case of C shows the opposite tendency to the above phenomena. In the locations of D and E, residual stress is uniform with negligible value, irrespectively along the location in thickness direction.

In the case of the transverse component of the residual stress, compressive residual stress in the surface of H-plate is turned into tensile residual stress in the middle of thickness at the locations of A and B as in Fig. 10. In the location of C, almost zero residual stress occurs at the surfaces of H-plate and maximum compressive residual stress occurs at the middle of the thickness. In the locations of D and E, compressive residual stress is produced uniformly.

5. Conclusion

The numerical simulation of welding process of H-plate was performed to understand the distribution of the residual stress. The residual stress measurement on the surface of H-plate by hole drilling method showed the validation of the numerical analysis.

As a whole, for the longitudinal component of the residual stress at the surface of H-plate, the trends of the experimental and numerical results are almost identical. In the case of the transverse component of the residual stress at the surface of H-plate, there is a little difference between the results of measurement and numerical simulation in the range from the center line of weld bead to 15 mm. This is thought that the difference is due to the insufficient material data, especially the varying properties according to the temperature.

The tendency of residual stress along the thickness is calculated by the finite element analysis. In the case of the longitudinal component of the residual stress in the weld zone and HAZ, the maximum tensile residual stress occurs at the center of thickness. In the case of the transverse component of the residual stress at the weld zone and HAZ, the compressive residual stress at the surface varies to the tensile residual stress at the center of thickness.

In the location of 10 mm apart from center line of weld bead, the trends of residual stress showed the opposite tendency to the above cases. In the locations of 15, 20 mm apart from center line of weld bead, the longitudinal and the transverse components of the residual stress is uniform along

the location in the thickness direction.

Acknowledgements

The authors are grateful for the support provided by a grant from the Korea Science & Engineering Foundation(KOSEF) and Safety and Structural Integrity Research Center at the Sungkyunkwan University.

References

ASTM 1995, "Standard Test Method for Determining Residual Stresses by the Hole-Drilling Strain-Gage Method," Annual book of ASTM standards ASTM E 837-92, 747-753.

Getnarski, R. B. 1986, *Thermal Stresses*, Nort h-Holland, New York.

Hibbitt H. D. and Marcal, P. V. 1973, "A Numerical thermo-Mechanical Model for the Welding and Subsequent Loading of a Fabricated Structure," *Computers and Structures*, Vol. 3, No. 5, pp. 1145~1174.

Jeon, S. Y. 1989, "Study of Residual Stress Measurement by Hole Drilling Method," Yeungnam Univ., A master's thesis.

Kabiri M., 1986, "Toward More Accurate Residual-Stress Measurement by the Hole-Drilling Method : Analysis of Relieved-Strain Coefficients," *Experimental Mechanics*, Vol. 24, No. 12, pp. 328~336.

Park S. D., 1994, *The Welding Engineering*, Won-Chang. Seoul.

Roelens J. B., Maltrud F. and Lu, J. 1994, "Determination of Residual Stresses in Submerged Arc Multi-pass Welds by Means of Numerical Simulation and Comparison with experimental Measurements," *Welding in the World*, Vol. 33, No. 3, pp. 152~159.

Schajer G. S., 1981, "Application of Finite Element Calculations to Residual Stress Measurements," *J. Eng. Mat. and Tech.*, 103, pp. 157~63.

Yang Y. S., Na S. J., Kim W. H., and Cho W. M., 1991, "Effect of Heat Treatments on Welding Residual Stresses of AISI4130 Steel," *KSME*, Vol 6, pp. 1982~1989.